



The role of acetylacetone in alkaline surface modification bath of electro-galvanized steel to enhance protective functioning of a hybrid silane coating

Sepideh Akbaripour Tafreshi Nejad^a, Eiman Alibakhshi^a, Bahram Ramezanzadeh^a, Fatemeh Marhamati^a, Marie-Georges Olivier^b, Mohammad Mahdavian^{a,*}

^a Institute for Color Science and Technology, Tehran, Iran

^b Department of Materials Science, Faculty of Engineering, University of Mons, Place de Parc, 20, 7000 Mons, Belgium

ARTICLE INFO

Keywords:

Surface modification
Electro-galvanized steel
Silane coating
Corrosion

ABSTRACT

The current work outlines the impact of acetylacetone (AcAc) in the alkaline surface treatment bath on durability and the anti-corrosion properties of electro-galvanized steel (EGS) coated with a hybrid silane composition. The surface characteristics of the EGS samples before and after modifications were appraised using atomic force microscopy, field emission scanning electron microscopy, and contact angle measurements confirming the changes in roughness, morphology and wettability properties imposed by surface treatments. To elucidate the chemical composition of the protecting layer developed on the surface of EGS, X-ray photoelectron spectroscopy was utilized which evidently endorsed forming a film consisting of zinc hydroxide, zinc oxide, and zinc acetylacetonate. The corrosion resistance of the specimens during immersion in 3.5 % NaCl medium was determined using electrochemical impedance spectroscopy and polarization experiments. The low-frequency impedance (at 0.01 Hz) of silane-coated samples modified in the optimal condition (0.5 M NaOH bath) in the presence and absence of AcAc was respectively ca. 15,900, 5800 Ω -cm². The electrochemical results corroborated the over-riding role of a trace amount of AcAc in the corrosion protection of silane-coated EGS samples. The novel surface treatment proposed in this work provides improved corrosion protection of silane coating on EGS having the lowest i_{corr} and presenting inhibition efficiency of 74 % in polarization experiment.

1. Introduction

Due to the widespread application of electro-galvanized steel (EGS), the improvement of its corrosion resistance is the subject of prodigious interest. Many attempts have been made to fulfill this objective [1–3]. The application scope of EGS encompasses a wide range of industries, including the automotive industry for car body panels [4,5]. Furthermore, considerable attention is switched to environmental alternatives to mitigate detrimental routes. In this regard, an appealing approach is to modify the EGS with silane-based coatings as the replacement of toxic chromate coatings [6–8].

Silane sol-gel coatings have evoked substantial interest due to the environmentally friendly feature, ease of application, firm adhesion between the resultant film and the substrate [3,9], and applicability to various substrates [10–12]. There are many factors affecting the performance of silane sol-gel films, including silane bath concentration,

alkoxysilane precursors, silane bath pH, and silane film curing temperature [13,14]. In fact, silane coatings provide barrier properties [3] which can be reinforced using various approaches [15–24].

Researchers have taken various approaches to reinforce corrosion resistance of silane coating by cerium nitrate [25], modified montmorillonite clay [26], and silica nanoparticles [27].

As a typical procedure, an alkaline modification has been employed to activate the surface of EGS before the application of silane coatings [11,17,28].

Due to the importance of uniform surface coverage, the process and substrate parameters that affect the wetting and the reactions between galvanized steel and the pretreatment bath should be taken into account. In fact, proper surface activation may lead to improved wettability and adhesion [29,30]. Saarimaa et al. investigated the surface activity of hot-dip galvanized steel after alkaline treatment. To this end, they used NaOH based solution [31].

* Corresponding author.

E-mail address: mahdavian-m@icrc.ac.ir (M. Mahdavian).

<https://doi.org/10.1016/j.porgcoat.2022.107048>

Received 5 February 2022; Received in revised form 15 June 2022; Accepted 14 July 2022

Available online 28 July 2022

0300-9440/© 2022 Elsevier B.V. All rights reserved.

Table 1

The details of surface pretreatment of different samples.

Sample	Details of pretreatment bath	Bath pH
Unmodified	No pretreatment was performed	–
0.1 M	0.1 M NaOH	12.5
0.1 M + AC	0.1 M NaOH (containing 2 wt% of AcAc)	9.5
0.5 M	0.5 M NaOH	13.1
0.5 M + AC	0.5 M NaOH (containing 2 wt% of AcAc)	13.0
1 M	1 M NaOH	13.3
1 M + AC	1 M NaOH (containing 2 wt% of AcAc)	13.1

The surface treatment of hot-dip galvanized steel was conducted by immersion in alkaline (sodium hydroxide) and acid (sulfuric acid) solutions, focusing on improvement in the wettability of the samples during the phosphating process. The results confirmed the alteration of surface composition after alkaline and acid treatments which have the potential to activate the surface prior to subsequent processes [32].

In a research conducted by Makarychev et al. hot-dip galvanized steel samples were subjected to alkaline treatment using 1 M KOH solution which in turn activated the surface prior to applying hybrid composite coating based on aminopropyltriethoxysilane [33].

Researchers also took advantages of alkaline treatment before applying different silane films including 3-mercaptopropyltrimethoxysilane (MTMO), 3-aminopropyltriethoxysilane (AMEO), and 3-glycidoxypropyltrimethoxysilane (GLYMO). For this end, 10 % (v/v) NaOH solution was used as the treatment bath for treating the electrogalvanized steel samples at 40 °C [34].

Deflorian et al. fabricated a corrosion protection system by depositing a silane layer consisting of a mixture of silanes (glycidoxypropyltrimethoxysilane, tetraethoxysilane, and methyltriethoxysilane) and an epoxy-polyester powder coating as the top layer, which can unveil the adhesion promoter role for the silane layer. Prior to silane deposition, the panels were degreased and treated in a commercial alkaline solution based on KOH, which ensured the etching and chemical activation of the surface [35].

However, the effect of surface modification conditions on the final silane coating properties has been rarely evaluated in the literature. The current work, for the first time, provides an in-depth study on the impact of different alkaline pretreatment bath compositions on the anti-corrosion properties of subsequent silane coating on EGS. In addition,

acetyl acetone (AcAc) was also added to the alkaline solutions. AcAc known as a strong chelating agent [36] is able to form zinc acetyl acetonate, known as an efficient corrosion inhibitor [37] on the EGS surface. Considering the chelating properties of AcAc, its effect in the alkaline surface treatment solutions was examined on the final silane coating protection behavior for the first time.

2. Experimental

2.1. Materials

EGS panels with a zinc layer thickness of $2.5 \pm 0.5 \mu\text{m}$ were obtained using a batch galvanization process performed by Gheteh Pooshesh Kar (Shahriar, Iran). The panels were chopped into 10 cm × 3 cm dimensions and used as the substrate. Tetraethyl orthosilicate (TEOS), 3-(chloropropyl)-trimethoxy silane (CPTMS), and acetyl acetone (AcAc) were supplied by GBXF Silicones Co., Merck, and Sigma, respectively. Nitric acid and NaOH (sodium hydroxide) were purchased from Mojalali Co.

2.2. Methodology

2.2.1. Chemical modification of EGS panels

First, the EGS panels were cleaned from contaminants using acetone and subsequently modified by NaOH medium at various concentrations (0.1, 0.5, and 1 M) with and without the addition of 2 wt% AcAc. The samples were modified at alkaline bath at 50 °C for 5 min. The modified panels were washed thoroughly using D.I water and dried by a compressed air stream. The details of samples pretreatment solutions are given in Table 1. According to this table presence of AcAc decreases alkalinity of the pretreatment solution, which is significant in the case of 0.1 M NaOH solution and negligible in the case of 0.5 M and 1 M NaOH solution.

2.2.2. Preparation of silane coating

The silane coating bath was prepared by mixing ethanol (73.7 % v/v), nitric acid (0.2 % v/v), D-I water (7.5 % v/v), TEOS (14.1 % v/v) and CPTMS 4.5 % (v/v). The aforementioned formulation was agitated overnight at room temperature (25 °C), which ensures the acceptable completion of the hydrolysis reaction (conversion of alkoxy groups to

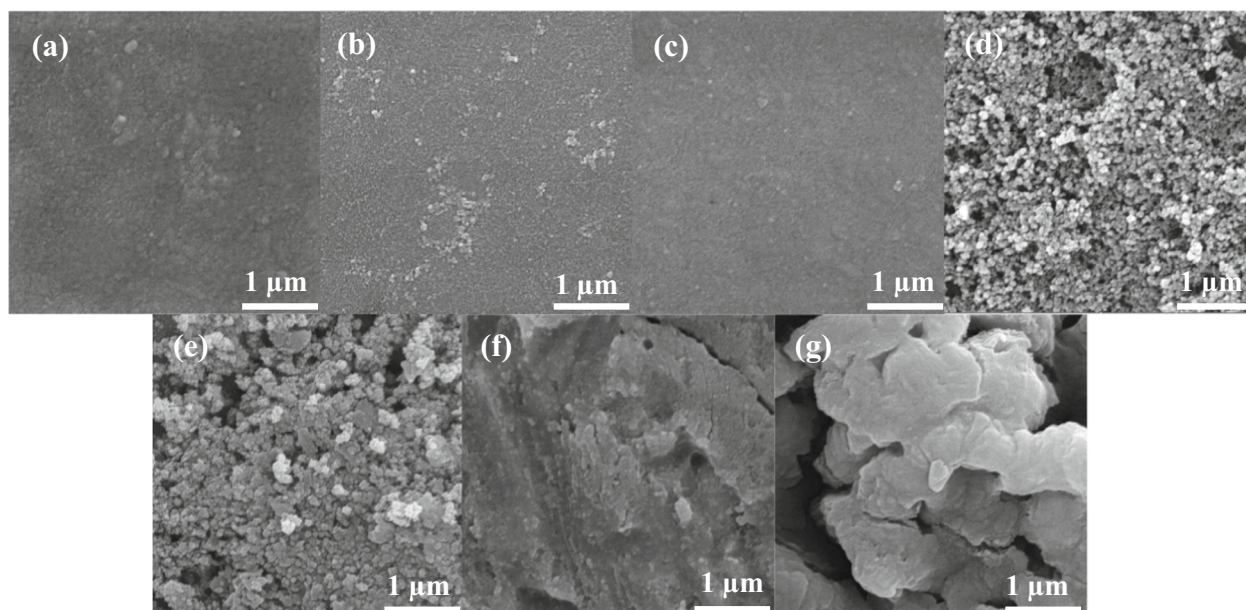


Fig. 1. FE-SEM micrographs of the modified surfaces prior to silane dip coating (a) unmodified, (b) 0.1 M, (c) 0.1 M + AC, (d) 0.5 M, (e) 0.5 M + AC, (f) 1 M, (g) 1 M + AC.

silanol groups). Afterward, EGS panels were dip-coated at a constant withdrawing speed of 100 mm/min. Then, the panels were allowed to dry at room temperature for 24 h and later the drying process was completed at a preheated oven at 150 °C for half an hour. Next, 1 cm × 1 cm area was selected as the exposure area, and the remaining area of the surface was covered using a sealant mixture.

2.3. Characterization

FE-SEM (field emission scanning electron microscopy) analysis was carried out in order to explore the morphological changes imposed by various alkaline modification conditions, to determine the surface coverage of silane films on EGS samples and the surface features after exposure to the corrosive environment. In this regard, Tescan Mira3 (Czech Republic) equipped with EDS (energy dispersive spectroscopy) was utilized.

The electrochemical behavior of the samples was assessed by EIS (electrochemical impedance spectroscopy) and polarization technique using an Ivium compactstat instrument performing on intact specimens subjected to 3.5 % NaCl medium. EIS was measured at open circuit potential applying 10 mV perturbation within 10 mHz–10 kHz frequency range. Polarization was measured at scan rate of +0.5 mV/s from –200 to +200 mV vs open circuit potential. Two replicas were tested through a three-electrode set-up constituted by a reference (saturated calomel), counter (platinum), and the working electrode (samples with 1 × 1 cm exposed area). Except for the initial fluctuation in the potential at the early stages of immersion, almost after 30 min, the open circuit potentials were stable.

To probe the chemical composition of the modified sample at the optimum condition by addressing the binding energies according to C1s line at 285.0 eV, XPS (X-ray photoelectron spectroscopy) was performed using X-ray 8025-BesTec XPS system employing Al K α radiation.

The surface morphology/roughness of the EGS after modification was investigated using DS 95-200 AFM (atomic force microscope). Tapping mode was utilized to record the AFM images. The wettability of the samples prior and after surface treatments was investigated through a contact angle measuring device by placing a 4 μ L drop on the surface and immediate image capturing. The measurements were repeated five times. The grazing incidence X-ray diffraction (GIXRD) analysis was performed by PHILIPS (Netherlands) to detect the phase-structure of the corrosion products formed on the silane coated samples after 72 h exposure to saline solution.

3. Results and discussion

3.1. Characterization of surface modified EGS

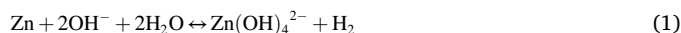
To pursue the alteration in surface morphology imposed by various modification conditions, the FE-SEM technique was exploited. The images of the samples after alkaline modification at various concentrations are shown in Fig. 1. The micrographs confirmed altering the surface morphology and the oxide film development on the surface in most of the modification conditions. In the case of the 0.5 M + AC sample, the oxide film was more compact. Moreover, increasing the concentration of NaOH in the modification bath caused more pronounced morphological changes to the surface by changing the chemical composition of the surface, simultaneously. In other words, the galvanized surface appears to have been deteriorated, and corrosion has occurred on the surface at higher modification concentrations (1 M, 1 M + AC). It can be deduced that by increasing the concentration of NaOH or addition of AcAc to the modifying bath, the surface appearance of EGS panels changes significantly, revealing the formation of a layer of corrosion products on the surface. The alkaline condition leads to the development of a layer of corrosion products. In such conditions, the zero-valent zinc converts to zincate according to Eq. (1) [38]. After surface neutralization, due to washing with D.I water zincate converts to zinc hydroxide according to

Table 2

Elemental weight percentage of the alkaline modified surfaces prior to silane dip coating.

Sample	Fe	O	Zn
Unmodified	–	3.4	96.6
0.1 M	–	12.8	87.2
0.1 M + AC	–	10.6	86.8
0.5 M	–	35.3	62.6
0.5 M + AC	–	37.5	64.7
1 M	89.2	3.6	7.2
1 M + AC	81.3	11.0	7.7

Eq. (2) [39].



The samples were also subjected to elemental analysis (EDS), and the findings are listed in Table 2. Accordingly, the weight percent of zinc sharply decreased compared to the reference sample, and a large amount of iron was detected on the surface. These outcomes are consistent with SEM images and indicate that the galvanized surface has been altered and destroyed at highly alkaline conditions. The milder modification conditions, i.e., 0.5 M, 0.5 M + AC resulted in a more oxygen content (as hydroxide or oxide) than the other samples. Such controlled oxidation can provide active places on the surface for the subsequent coating.

AFM gives ideas about the extent of corrosion attacks on the surface, examining the roughness of the specimens. The changes on the surface topography imparted by various modifications were screened in Figs. S1 and S2. The surface of the unmodified galvanized steel is smooth, while surface modification has increased the surface roughness. Fig. S2h summarizes the different parameters, including Sz (maximum height), Sa (arithmetical mean height), and Sq (root mean square height). Increasing the concentration of NaOH led to an increase in surface roughness of the samples, which is in reasonable conformity with FE-SEM outcomes. The 1 M + AC surface modification reveals the greatest values of roughness parameters which might be due to greater etching effects at the high alkaline condition and the chelation of AcAc with Fe²⁺ and Zn²⁺ cations. The formation of such compounds on the surfaces during the modification process justifies the significant changes in the aforementioned parameters [40].

Fig. 2 depicts the contact angle (θ) of water droplets on the surfaces of unmodified and modified samples. The θ indicates the wettability at the solid-liquid interface, and the smaller θ refers to better spreading ability. The water contact angle is also attributed to the hydrophilic/hydrophobic nature on the surface. The water contact angle (91.8 \pm 2.3) of the unmodified EGS is much larger than the modified samples, which indicates an improvement in the wettability of the surface upon alkaline pretreatment. According to Fig. 2, the 0.5 M + AC surface-modified sample has the lowest θ value. Wettability of the metal surface is one of the important factors affecting silane coatings' performance. Higher wettability reflects higher hydrophilicity originated from polar groups formation on the surface. Wettability not only affects uniform silane film formation on the surface but also affects its chemical reaction with the EGS surface. The presence of sufficient polar groups, e.g., OH groups, on the surface is essential for the condensation reaction of silanol groups of silane coating to form Si-O-Zn bonds. According to the results of surface roughness, contact angle, and elemental analysis, 0.5 M + AC sample was selected as the best surface modification. The zinc layer was significantly destroyed due to the severe corrosivity of 1 M NaOH.

XPS test was carried out to determine the composition of hydroxide/oxide compounds in the surface film. Supplementary Information (Fig. S3) gives the essence of Zn, O, and C elements on the surface of 0.5 M + AC sample in its wide-scan XPS spectra. Consistent with the EDS outcomes, iron was not observed on this sample. The high-resolution O1

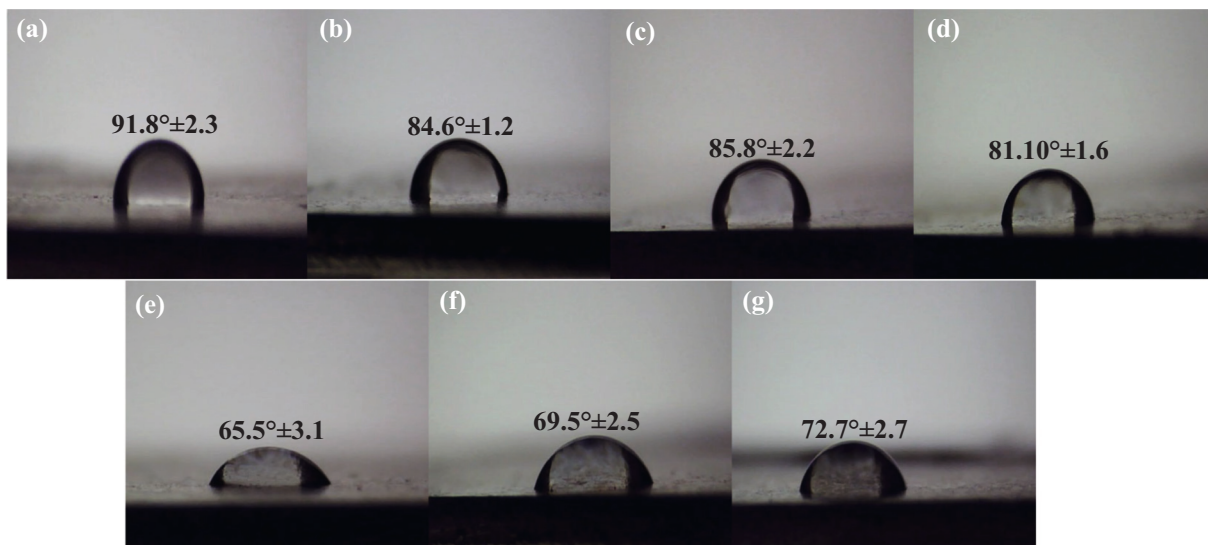


Fig. 2. Contact angles measurements results of (a) unmodified, (b) 0.1 M, (c) 0.1 M + AC, (d) 0.5 M, (e) 0.5 M + AC, (f) 1 M, (g) 1 M + AC.

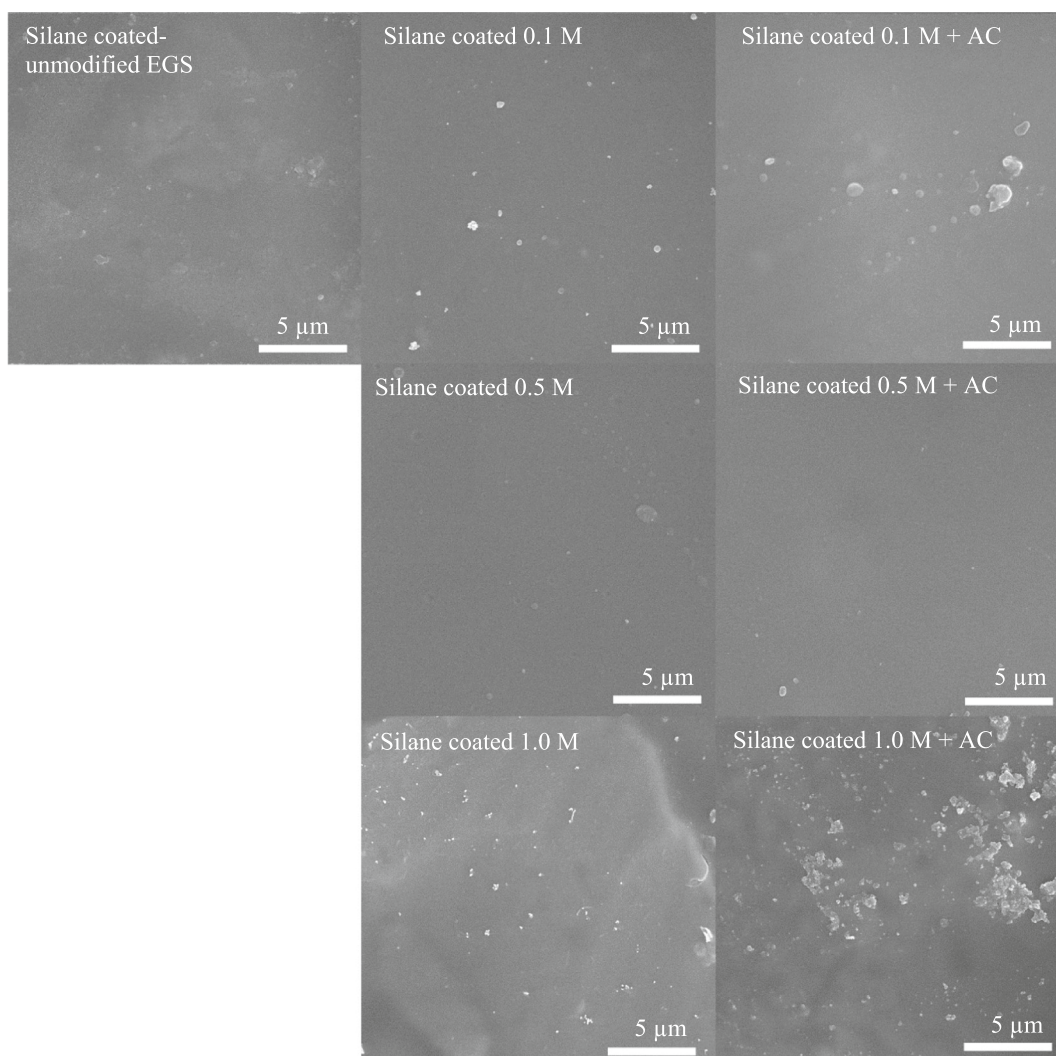


Fig. 3. FESEM images of silane-coated samples applied on EGS surface modified at different conditions.

Table 3

EDS elemental composition (wt%) of silane-coated samples applied on EGS surface modified at different conditions.

	C	O	Fe	Zn	Si
Silane coated-unmodified EGS	9.1	15.4	0	32.2	43.3
Silane coated 0.1 M	9.1	14.6	0	32.4	43.9
Silane coated 0.1 M + AC	8.7	14.7	0	33.2	43.4
Silane coated 0.5 M	12.4	19.7	0	17.4	50.5
Silane coated 0.5 M + AC	12.9	18.9	0	17.1	51.1
Silane coated 1.0 M	8.9	20.3	31.6	3.9	35.3
Silane coated 1.0 M + AC	8.3	19.9	30.7	3.2	37.9

s spectrum depicts the binding energies at 530, 531.8, and 533.1 eV, which correspond to the acetylacetonate, ZnO, and Zn(OH)₂ bands, respectively [41]. The high-resolution Zn 2p_{3/2} spectrum shows similar oxy/hydroxide bands at around 1021.5, 1022.2, and 1022.5 eV, respectively [42]. This suggests that alkaline modification in the presence of AcAc formed a film of zinc hydroxide, zinc oxide, and zinc acetylacetonate. Active surface functionality on the EGS surface can form covalent bonding with the upcoming silane coating.

3.2. Silane coatings applied on surface-modified EGS

Silane was coated on the surface-modified and unmodified samples. The proposed reaction of silane compounds is hydrolysis of alkoxy groups in the first step to form silanols groups and condensation of silanol groups and surface OH groups in the second step [43]. The chloride group is also susceptible to hydrolysis forming hydroxyl function on the alkyl chain of silane compound [44]. This reaction involves in release of HCl which dropped the pH from 3.5 to 3.0 after hydrolysis period. The overall silane reactions to form silane coating are depicted in the Supplementary Information (Fig. S4). The surface coverage of silane coatings formed on the EGS samples was assessed by FESEM-EDS. The results are provided in Fig. 3 and Table 3. According to the FESEM micrographs, the silane film formation on the unmodified surface was not uniform. The treatments by 0.1 M NaOH (with and without AcAc), led to a better uniformity compared to the unmodified sample. The highest uniformity with silane coating was obtained on the substrate treated by using 0.5 M NaOH (with and without AcAc). The treatments by 1 M NaOH (with and without AcAc) resulted in a very irregular surface film, probably due to the deterioration of the galvanized layer. Elemental analysis showed that the highest Si content on the surface could be

achieved by treatment at 0.5 M NaOH (in the presence and absence of AcAc), which can be attributed to the better uniformity and integrity of the silane films formed on these samples. It was depicted that surface treatment with alkaline solution improves the wettability of the surface (Fig. 2), which can subsequently result in more silane coating build-up. In contrast, low surface wettability usually leads to repelling of the silane coating, resulting in inhomogeneous surface coverage.

The corrosion resistance of silane coatings was evaluated in a 3.5 % sodium chloride solution through visual observation, EIS, and polarization measurements. Fig. 4 displays the visual observation of the silane coated samples after immersion for 12 days. After the prolonged immersion period of 12 days, the optimal sample was only covered with white rust, while remarkable corrosion products were detectable in the case of unmodified EGS, silane coated-unmodified EGS, silane-coated 1 M, and silane-coated 1 M + AC samples.

The silane-coated samples (with the exposure area of 1 × 1 cm) were analyzed using EIS measurements during various immersion times, i.e., 1 h, 3 h, 24 h, 48 h, and 72 h, to evaluate their corrosion protection on the modified EGS substrates. Fig. 5 displays the Nyquist diagrams for the silane-coated samples. Impedance module and Bode-phase diagrams are given in Supplementary Information (Figs. S5 and S6), respectively.

Bode-phase diagrams may be used to explain corrosion processes that take place at the coating and metal-solution interface [45]. In the case of the bare EGS sample (without coating), a two-time constant has been detected, which is connected to the electrical double layer and oxide layer. At the same time, two- or three-time constants have been found for the most silane-coated samples. These high-frequency, medium-frequency, and low-frequency time constants are correlated to the silane coating, the oxide layer (resulted from surface modification or oxidation of metal surface during corrosion test), and electrical double layer, respectively [46,47].

The low-frequency impedance in Bode and capacitive-loop diameter in the Nyquist diagrams indicate the total resistance of a coating system. These parameters can be thought of as a precise criterion for assessing corrosion resistance [48,49]. The low-frequency impedance values ($|Z|$ at 10 mHz) of silane coated samples are provided in Fig. 6. The blank sample has the smallest capacitive-loop size and lowest low-frequency impedance modulus. This behavior is caused by the occurrence of corrosion and deterioration of the EGS surface. By application of the silane coatings, overall resistance of the samples has been improved. Silane coatings on the surface-modified samples showed a resistance increase compared to the silane coating on the unmodified surface. In

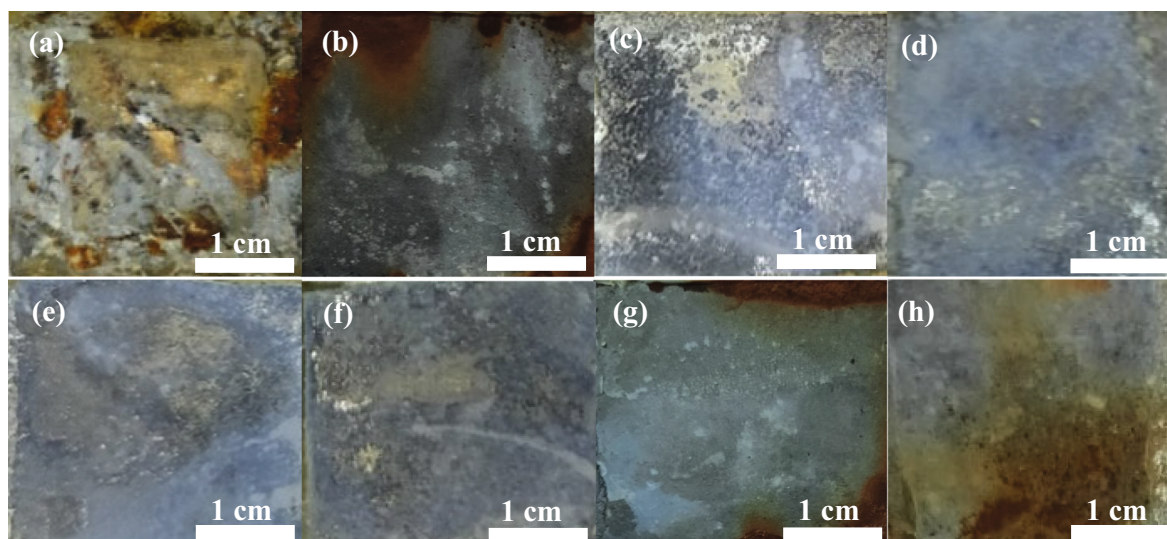


Fig. 4. The EGS panels after immersion in 3.5 % NaCl solution for 12 days (a–h); (a) uncoated-unmodified EGS, (b) silane coated-unmodified EGS, (c) silane coated 0.1 M, (d) silane coated 0.1 M + AC, (e) silane coated 0.5 M, (f) silane coated 0.5 M + AC, (g) silane coated 1M, (h) silane coated 1 M + AC.

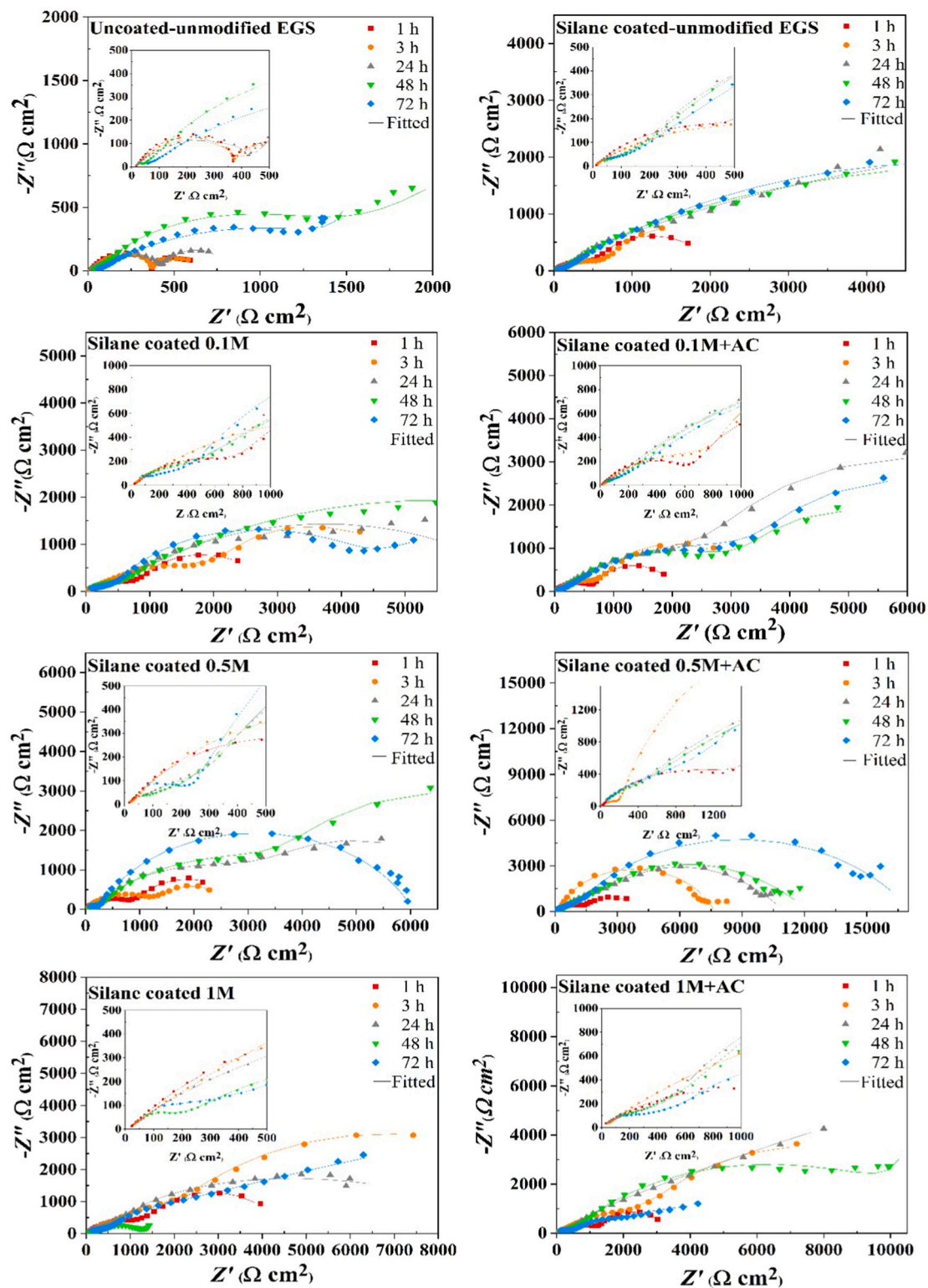


Fig. 5. The Nyquist diagrams of silane-coated samples at different immersion times.

addition, the surface modification in the presence of AcAc outperforms samples without it in terms of corrosion protection. Among them, the best performance belongs to the silane-coated 0.5 M + AC sample. In this case, the total value rises and reaches its limit after 72 h. This is the obvious evidence of the interaction of zinc and AcAc at the surface-active areas.

In order to conduct an in-depth study into the obtained results, the

data were fitted using an appropriate electrical equivalent circuit (EEC). Supplementary information (Fig. S7) shows the EECs that were utilized to match the EIS data.

Considering the non-ideal action of the samples, CPE (constant phase element) was provided in the circuits consisting of Y (admittance) and n (exponent) elements. The CPE impedance is given by the Eq. (3), where ω is the angular frequency and j is the imaginary unit [50].

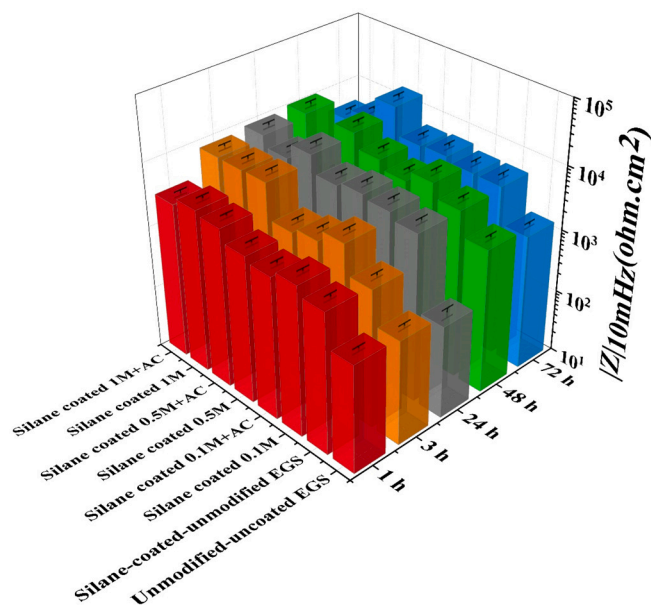


Fig. 6. The low-frequency impedance of silane-coated samples at different immersion times.

$$Z_{CPE} = \frac{1}{Y_0(j\omega)^n} \quad (3)$$

In fact, CPE is considered due to the lack of surface homogeneity or lack of intactness of the inhibitive layer [51,52]. The modeled circuit for the EGS shows five fragments, including electrolyte resistance (R_s), charge transfer resistance (R_{ct}), double-layer constant phase element (CPE_{dl}), R_{ox} (oxide layer resistance) and CPE_{ox} (oxide layer constant phase element), as shown in Fig. S7a. Fig. S7b reveals a second time constant similar to Fig. S7a, except that R_{ox} (oxide layer resistance) and CPE_{ox} (oxide layer constant phase element) were substituted by R_c (coating resistance) and CPE_c (coating constant phase element). Fig. S7c provides different moduli which are added to the circuit used to fit three-time constant frequency responses. The quantitative outcomes are presented in Supplementary information (Table S1).

In the case of the neat EGS sample, the total resistance ($R_{ct} + R_{ox} + R_c$) is lower than those of the other samples during the immersion stages. For this sample, the total resistance increases up to 48 h, and later on, begins to decline. The total resistance values of the silane on the unmodified sample are slightly higher than the neat EGS sample (blank), meaning that the application of the coating has increased the corrosion resistance. However, the total resistance values are higher as alkaline modifications are applied to EGS surfaces. The oxide layer appears to be the most important contributor to the corrosion resistance. The oxide layer resistance of the silane-coated 0.5 M + AC sample is higher than that for the other surface-modified silane-coated specimens at the end of the exposure time. For a case in point (silane-coated 0.5 M + AC), total resistance values increased with time up to 72 h. Whereas the other pre-modified silane coated samples showed total resistance slow increment and later on started a reduction. Hence, this behavior of silane-coated 0.5 M + AC concludes a good protecting performance. This may be due to zinc and AcAc interacting at the surface-active regions.

Changes in coating resistance (R_c) give information on the barrier action of the coating [42]. Coating resistance for silane-coated 0.5 M + AC is the highest among the silane coated samples across the whole immersion duration. It is also understandable from the results that the reduction in initial film resistance occurs due to the penetration of electrolyte into the coating. In addition, corrosion reaction beneath the coating can damage the coating integrity during immersion time leading to a decrease in coating resistance. This outcome is a sign of gradual electrolyte uptake and loss of its barrier protection.

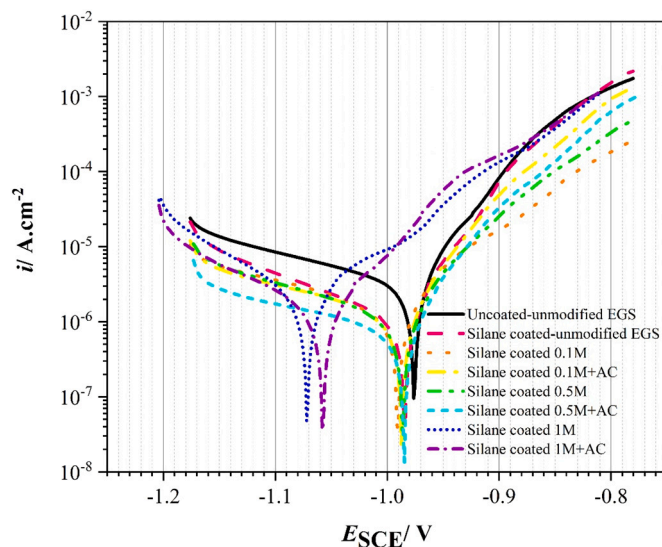


Fig. 7. Potentiodynamic polarization plot of the silane-coated samples after 72 h immersion.

Table 4

The values of corrosion current density, corrosion potential, and Tafel slopes for different samples after 72 h immersion in 3.5 wt% NaCl solution.

Sample	E_{corr} (V/SCE)	i_{corr} ($\mu\text{A}/\text{cm}^2$)	η (%)
Uncoated-unmodified EGS	-0.976 ± 0.10	3.5 ± 0.3	–
Silane coated-unmodified EGS	-0.984 ± 0.08	1.6 ± 0.2	54
Silane coated 0.1 M	-0.99 ± 0.05	1.5 ± 0.2	57
Silane coated 0.1 M + AC	-0.987 ± 0.03	1.4 ± 0.2	60
Silane coated 0.5 M	-0.986 ± 0.03	1.4 ± 0.1	60
Silane coated 0.5 M + AC	-0.985 ± 0.02	0.9 ± 0.1	74
Silane coated 1 M	-1.08 ± 0.05	2.3 ± 0.1	34
Silane coated 1 M + AC	-1.07 ± 0.05	1.5 ± 0.2	57

It is certifying from the EIS results that silane-coated 0.5 M + AC demonstrates the best corrosion protection among the pre-modified silane coated samples, which is consistent with the samples' visual appearance (Fig. 4).

Comparison of CPE values of the samples (Table S1) can also provide information about the electrochemical behavior of surface treated EGS samples. The silane coated unmodified EGS sample at the end of the evaluation period (72 h immersion) showed that the $Y_{0,c}$ equal to $110.9 \mu\text{s}^n \cdot \Omega^{-1} \cdot \text{cm}^{-2}$, which was decreased for the surface modified samples in 0.1 M and 0.5 M NaOH. Such a decrease can be attributed to a lower water uptake of these coatings and less damage induced by corrosion to the silane coatings. Surface treatment at 1 M NaOH led to an increase in CPE admittance, reflecting the negative effect of surface treatment at high alkaline conditions.

To achieve a deeper understanding of the protection process, the potentiodynamic polarization test was used. Fig. 7 displays the representative polarization scans of the prepared samples after 72 h dipping in the NaCl solution. Tafel extrapolation model fitting was used to measure i_{corr} (corrosion current density), and E_{corr} (corrosion potential). Inhibition efficiency of the samples after 72 h of immersion was calculated using Eq. (4) [53], which along with the data obtained from fitting the polarization curves, are tabulated in Table 4.

$$\eta = \left(1 - \frac{i_{corr}}{i_{corr}^0}\right) \times 100 \quad (4)$$

where i_{corr} and i_{corr}^0 represent the corrosion current density of the pre-treated/silane-coated samples and corrosion current density of the blank sample, respectively.

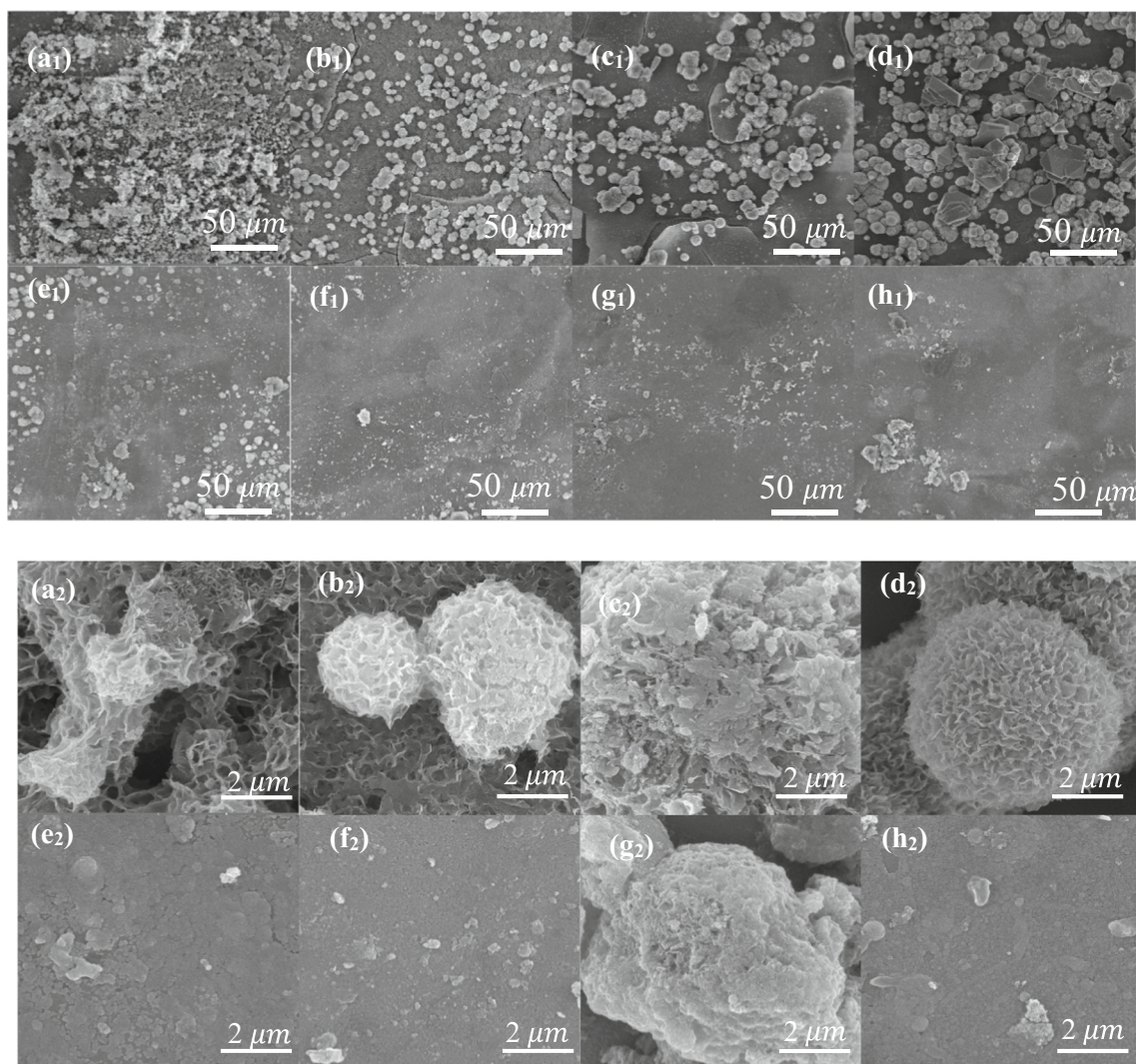


Fig. 8. FE-SEM micrographs of the silane coated samples after exposing to 3.5 % NaCl solution (a₁,a₂) uncoated-unmodified EGS (b₁,b₂) silane coated-unmodified EGS, (c₁, c₂) silane coated 0.1 M, (d₁,d₂) silane coated 0.1 M + AC, (e₁,e₂) silane coated 0.5 M, (f₁,f₂) silane coated 0.5 M + AC, (g₁,g₂) silane coated 1 M, (h₁,h₂) silane coated1M + AC.

Looking at Fig. 7 and Table 4, depression of anodic and cathodic branches has been occurred by applying the silane coating and surface modification of EGS. The lower i_{corr} value for the silane-coated unmodified sample compared to the blank sample indicates the protecting ability of the silane film. Compared with the unmodified sample, the modified samples at 0.1 and 0.5 M NaOH revealed a significant reduction in i_{corr} where the treatment at 0.5 M NaOH, especially in the presence of AcAc, depicted the most remarkable impact on the corrosion rate. The results obtained from Eq. (4) indicated that the highest inhibition efficiency was achieved by the silane-coated 0.5 M + AC sample. Upon surface modification with 1 M NaOH, the shift of corrosion potential to more negative values has been taken place, which can be attributed to the presence of an excess of hydroxide at the interface, even after washing, which led to an increase in the interface pH. Such an increase in pH shifts the electrode potential to more negative values on the remaining zinc layer, according to Eq. (5) [54], and on the Fe surface where the zinc layer is destroyed, according to Eq. (6) [55].



$$E = -0.439 - 0.0591\text{pH.}$$



$$E = -0.08 - 0.0591\text{pH.}$$

The best protection ability was confirmed by the lowest i_{corr} of silane coated 0.5 M + AC sample. Based on the electrochemical results, the surface treatment at 0.1 M NaOH generates hydroxide groups on the surface, resulting in improved protection. The superior protection was achieved in the presence of 0.5 M NaOH providing sufficient surface -OH groups. An increase in alkalinity up to 1 M NaOH, led to a reduction in protection compared to 0.5 M NaOH, which could be originated from the presence of excess unneutralized OH^- anions in the surface film and a strong attack on the zinc layer. Improved protection with surface treatment in the presence of AcAc could be connected to its strong chelation with zinc cations on the surface.

The status of the silane coated samples after 72 h immersion was further inspected by SEM and outcomes are depicted in Fig. 8.

As seen in Fig. 8a and b, the metal surface of the blank and unmodified (Silane coated-Unmodified EGS) samples has formed a high growth of corrosion products. As a result of the extensive metal dissolution, EGS, without any modification, is determinedly corroded. The surface morphology is totally different for the modified samples. In other words, a denser morphology with fewer corrosion attacks was observed for these samples than the blank and unmodified samples. The silane-coated 0.5 M + AC sample illustrated the best integrity among the test samples indicating the least corrosion attacks which was in line with the

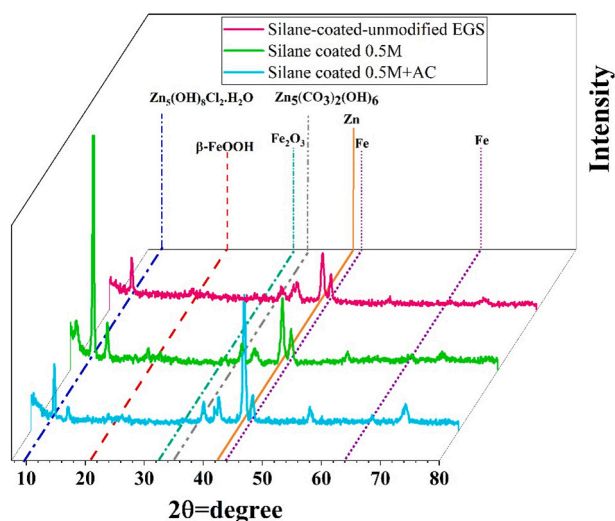


Fig. 9. GIXRD pattern of the silane coated samples after 72 h exposure to 3.5 % NaCl solution.

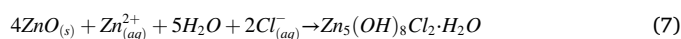
electrochemical test results.

3.3. Impact of AcAc in the pretreatment solution

AcAc is a robust chelating agent which can form zinc acetylacetonate. Its ability to create zinc acetylacetonate on the galvanized steel surface was proved by XPS (see Section 3.1). In the absence of zinc acetylacetonate, the only possible reaction on the surface of galvanized steel is the formation of zinc hydroxide, as per Eq. (2). Although the hydroxide functionalities on the galvanized steel surface are required to favor the condensation reactions with silanol groups of silane coatings, due to its high basic character (zinc hydroxide has a pKa of 29.0 [56]), it has low stability at pH \approx 3–4 (the silane bath pH). AcAc has a weak basic character (pKa = 9.07 [57]), so its complex with zinc can be more stable at low pHs as pH \approx 3–4 compared to zinc hydroxide. In other words, with partial substitution of zinc hydroxide with zinc acetylacetonate in the presence of AcAc, the galvanized steel surface becomes more resistant to mildly acidic conditions. In addition, zinc acetylacetonate has already been known as a corrosion inhibitor [37]. The presence of zinc acetylacetonate-rich thin layer on the galvanized steel could serve as a corrosion inhibitor reservoir for the subsequent corrosion attacks especially when the galvanized layer is damaged. Utilization of AcAc in the alkaline pretreatment solutions of galvanized steel can improve the quality of the surface film for the application of subsequent coatings.

To gain deep understanding of the effect of AcAc on the protective function of silane coated samples, the samples were examined by GIXRD analysis. The result of GIXRD analysis of silane coated samples after 72 h exposure to the saline solution is plotted in Fig. 9. The peaks appeared at $2\theta \approx 22^\circ$ and $2\theta \approx 33^\circ$ can be ascribed to ferric hydroxide and ferric oxide related compounds [58], respectively which are not detected in case of silane coated 0.5 M + AC sample. This phenomenon indicates the

corrosion mitigation as a result of surface treatment. The pure Fe peaks (reference code: 96-900-6598) is evident in the spectrum attributed to the Fe substrate beneath the Zn layer. The peaks appeared at $2\theta \approx 43.5^\circ$ is ascribed to Zn (101) according to 96-901-2436 reference code which is intensified in the patterns obtained from pretreated samples and can be interpreted by less deterioration of zinc layer. The Zn₅(OH)₈Cl₂·H₂O peak (11°) [59] is escalated in Silane-coated 0.5 M sample in respect to available zinc oxide compounds produced by alkaline treatment according to the reaction shown in Eq. (7) [60]. The intensity of the aforementioned peak was weakened in Silane coated 0.5 M + AC sample due to the formation of zinc acetyl acetonate which can act as an effective corrosion inhibitor.



In order to gain insight into the exerted impact of pretreatment used in the current study, the obtained corrosion impedances were compared with the relevant articles considering the application of silane hybrid coating on different pre-treated surfaces using alkaline pretreatment conditions. The results are summarized in Table 5. It can be concluded from the results that the optimum pretreatment used in this study (0.5 M + AcAc) has a comparable impact on the performance of silane coating for corrosion protection of galvanized steel.

4. Conclusion

Prior to applying the silane coating, the EGS surface was modified using NaOH alkaline solutions with or without acetylacetonate (AcAc) to improve the corrosion protection of the metallic substrate. Surface modification at 1 M NaOH showed severe corrosion attacks on the surface, leading to the deterioration of zinc layer integrity. However, surface modification at lower concentrations resulted in no side effect on zinc layer integrity while increasing the surface oxygen content. The treatment at 0.5 M NaOH and AcAc produced a significant amount of oxygen (as hydroxide or oxide) on the surface film, while the chelation of AcAc with zinc was confirmed with XPS. The low-frequency impedance (at 0.01 Hz) of silane-coated samples modified in 0.5 M NaOH bath in the presence and absence of AcAc was respectively ca. 15,900, 5800 $\Omega \cdot \text{cm}^2$. The electrochemical findings confirmed the overriding function of a low amount of AcAc in the alkaline surface treatment bath on the corrosion resistance of the silane coating.

Partial substitution of zinc hydroxide with zinc acetylacetonate in the presence of AcAc, led to higher stability of galvanized steel surface in mildly acidic conditions, which is a typical medium for silane coatings. Considering the results obtained, the treatment method can be a proper substitute for the available alkaline solutions to enhance the corrosion protection performance of silane coatings.

Declaration of competing interest

The authors declare that they have no known competing financial interests or personal relationships that could have appeared to influence the work reported in this paper.

Table 5

Comparison of the pre-treatment effect on the anti-corrosion performance of different substrates coated with silane coating.

Substrate	Pre-treatment condition	Immersion time	Low frequency impedance (blank sample)	Low frequency impedance (pre-treated and silane coated sample)	Reference
Galvanized steel	0.5 M + AcAc (5 min @ 50 °C)	72 h	1.4 k Ω cm ²	15.9 k Ω cm ²	–
Magnesium	3 M NaOH (48 h)	1 h	1 k Ω cm ²	6 k Ω cm ²	[61]
Aluminium alloy AA2024-T3	0.5 M NaOH (5 min)	72 h	5 k Ω cm ²	40 k Ω cm ²	[62]
Galvanized steel	Alkaline cleaner	Initial immersion stage	500 Ω cm ²	5.5 k Ω cm ²	[63]

Appendix A. Supplementary data

Supplementary data to this article can be found online at <https://doi.org/10.1016/j.porgcoat.2022.107048>.

References

- [1] B. Ramezanzadeh, M. Attar, M. Farzam, Corrosion performance of a hot-dip galvanized steel treated by different kinds of conversion coatings, *Surf. Coat.* 205 (2010) 874–884, <https://doi.org/10.1016/j.surfcoat.2010.08.028>.
- [2] D. Xue, W.J. Van Ooij, Corrosion performance improvement of hot-dipped galvanized (HDG) steels by electro-deposition of epoxy-resin-ester modified bis-[triethoxy-silyl] ethane (BTSE) coatings, *Prog. Org. Coat.* 76 (2013) 1095–1102, <https://doi.org/10.1016/j.porgcoat.2013.03.004>.
- [3] W. Trabelsi, E. Triki, L. Dhoubi, M. Ferreira, M. Zheludkevich, M. Montemor, The use of pre-treatments based on doped silane solutions for improved corrosion resistance of galvanised steel substrates, *Surf. Coat.* 200 (2006) 4240–4250, <https://doi.org/10.1016/j.surfcoat.2005.01.044>.
- [4] J. Angeli, T. Kaltenbrunner, F. Androsch, Quantitative depth-profiling with GDOS: application to ZnNi-electroplated steel sheets, *Fresenius J. Anal. Chem.* 341 (1991) 140–144, <https://doi.org/10.1007/BF00322125>.
- [5] H. Jiang, X. Chen, H. Wu, C. Li, Forming characteristics and mechanical parameter sensitivity study on pre-phosphated electro-galvanized sheet steel, *J. Mater. Process. Technol.* 151 (2004) 248–254, <https://doi.org/10.1016/j.jmatprotec.2004.04.069>.
- [6] K. Gang, L. Jintang, W. Haijiang, Post treatment of silane and cerium salt as chromate replacers on galvanized steel, *J. Rare Earths* 27 (2009) 164–168, [https://doi.org/10.1016/S1002-0721\(08\)60213-6](https://doi.org/10.1016/S1002-0721(08)60213-6).
- [7] F. Deflorian, S. Rossi, L. Fedrizzi, Silane pre-treatments on copper and aluminium, *Electrochim. Acta* 51 (2006) 6097–6103, <https://doi.org/10.1016/j.electacta.2006.02.042>.
- [8] M. Montemor, W. Trabelsi, S. Lamaka, et al., The synergistic combination of bis-silane and CeO₂-ZrO₂ nanoparticles on the electrochemical behaviour of galvanised steel in NaCl solutions, *Electrochim. Acta* 53 (2008) 5913–5922, <https://doi.org/10.1016/j.electacta.2008.03.069>.
- [9] M. Juan-Díaz, M. Martínez-Ibáñez, M. Hernández-Escolano, et al., Study of the degradation of hybrid sol-gel coatings in aqueous medium, *Prog. Org. Coat.* 77 (2014) 1799–1806, <https://doi.org/10.1016/j.porgcoat.2014.06.004>.
- [10] M. Montemor, M. Ferreira, Electrochemical study of modified bis-[triethoxysilylpropyl] tetrasulfide silane films applied on the AZ31 mg alloy, *Electrochim. Acta* 52 (2007) 7486–7495, <https://doi.org/10.1016/j.electacta.2006.12.086>.
- [11] M. Montemor, A. Cabral, M. Zheludkevich, M. Ferreira, The corrosion resistance of hot dip galvanized steel pretreated with bis-functional silanes modified with microsilica, *Surf. Coat.* 200 (2006) 2875–2885, <https://doi.org/10.1016/j.surfcoat.2004.11.012>.
- [12] A. Franquet, H. Terryn, J. Vereecken, Study of the effect of different aluminium surface pretreatments on the deposition of thin non-functional silane coatings, *Surf. Interface Anal.* 36 (2004) 681–684, <https://doi.org/10.1002/sia.1735>.
- [13] A. Franquet, C. Le Pen, H. Terryn, J. Vereecken, Effect of bath concentration and curing time on the structure of non-functional thin organosilane layers on aluminium, *Electrochim. Acta* 48 (2003) 1245–1255, [https://doi.org/10.1016/S0013-4686\(02\)00832-0](https://doi.org/10.1016/S0013-4686(02)00832-0).
- [14] A.-P. Romano, M. Fedel, F. Deflorian, M.-G. Olivier, Silane sol-gel film as pretreatment for improvement of barrier properties and filiform corrosion resistance of 6016 aluminium alloy covered by cathodic coating, *Prog. Org. Coat.* 72 (2011) 695–702, <https://doi.org/10.1016/j.porgcoat.2011.07.012>.
- [15] M. Montemor, M. Ferreira, Analytical characterization of silane films modified with cerium activated nanoparticles and its relation with the corrosion protection of galvanised steel substrates, *Prog. Org. Coat.* 63 (2008) 330–337, <https://doi.org/10.1016/j.porgcoat.2007.11.008>.
- [16] M. Montemor, R. Pinto, M. Ferreira, Chemical composition and corrosion protection of silane films modified with CeO₂ nanoparticles, *Electrochim. Acta* 54 (2009) 5179–5189, <https://doi.org/10.1016/j.electacta.2009.01.053>.
- [17] F. Deflorian, S. Rossi, M. Fedel, C. Motte, Electrochemical investigation of high-performance silane sol-gel films containing clay nanoparticles, *Prog. Org. Coat.* 69 (2010) 158–166, <https://doi.org/10.1016/j.porgcoat.2010.04.007>.
- [18] M.-G. Olivier, M. Fedel, V. Sciamanna, et al., Study of the effect of nanoclay incorporation on the rheological properties and corrosion protection by a silane layer, *Prog. Org. Coat.* 72 (2011) 15–20, <https://doi.org/10.1016/j.porgcoat.2010.11.022>.
- [19] L.M. Palomino, P.H. Suegama, I.V. Aoki, M.F. Montemor, H.G. De Melo, Electrochemical study of modified non-functional bis-silane layers on Al alloy 2024-T3, *Corros. Sci.* 50 (2008) 1258–1266, <https://doi.org/10.1016/j.corsci.2008.01.018>.
- [20] M. Ferreira, R. Duarte, M. Montemor, A. Simões, Silanes and rare earth salts as chromate replacers for pre-treatments on galvanised steel, *Electrochim. Acta* 49 (2004) 2927–2935, <https://doi.org/10.1016/j.electacta.2004.01.051>.
- [21] E. Alibakhshi, E. Ghasemi, M. Mahdavian, B. Ramezanzadeh, Fabrication and characterization of layered double hydroxide/silane nanocomposite coatings for protection of mild steel, *J. Taiwan Inst. Chem. Eng.* 80 (2017) 924–934, <https://doi.org/10.1016/j.jtice.2017.08.015>.
- [22] B. Ramezanzadeh, M. Akbarian, M. Ramezanzadeh, M. Mahdavian, E. Alibakhshi, P. Kardar, Corrosion protection of steel with zinc phosphate conversion coating and post-treatment by hybrid organic-inorganic sol-gel based silane film, *J. Electrochem. Soc.* 164 (2017) C224, <https://doi.org/10.1149/2.0491706jes>.
- [23] R. Samiee, B. Ramezanzadeh, M. Mahdavian, E. Alibakhshi, Corrosion inhibition performance and healing ability of a hybrid silane coating in the presence of praseodymium (III) cations, *J. Electrochem. Soc.* 165 (2018) C777, <https://doi.org/10.1149/2.0841811jes>.
- [24] R. Samiee, B. Ramezanzadeh, M. Mahdavian, E. Alibakhshi, Assessment of the smart self-healing corrosion protection properties of a water-base hybrid organo-silane film combined with non-toxic organic/inorganic environmentally friendly corrosion inhibitors on mild steel, *J. Clean. Prod.* 220 (2019) 340–356, <https://doi.org/10.1016/j.jclepro.2019.02.149>.
- [25] W. Trabelsi, P. Cecilio, M. Ferreira, M. Montemor, Electrochemical assessment of the self-healing properties of ce-doped silane solutions for the pre-treatment of galvanised steel substrates, *Prog. Org. Coat.* 54 (2005) 276–284, <https://doi.org/10.1016/j.porgcoat.2005.07.006>.
- [26] C. Motte, M. Poelman, A. Roobroeck, M. Fedel, F. Deflorian, M.-G. Olivier, Improvement of corrosion protection offered to galvanized steel by incorporation of lanthanide modified nanoclays in silane layer, *Prog. Org. Coat.* 74 (2012) 326–333, <https://doi.org/10.1016/j.porgcoat.2011.12.001>.
- [27] S. Akhtar, A. Matin, A.M. Kumar, A. Ibrahim, T. Laoui, Enhancement of anticorrosion property of 304 stainless steel using silane coatings, *Appl. Surf. Sci.* 440 (2018) 1286–1297, <https://doi.org/10.1016/j.apsusc.2018.01.203>.
- [28] N. Parhizkar, B. Ramezanzadeh, T. Shahrabi, Corrosion protection and adhesion properties of the epoxy coating applied on the steel substrate pre-treated by a sol-gel based silane coating filled with amino and isocyanate silane functionalized graphene oxide nanosheets, *Appl. Surf. Sci.* 439 (2018) 45–59, <https://doi.org/10.1016/j.apsusc.2017.12.240>.
- [29] K. Kaluzny, Why some metals and alloys are more difficult to pretreat than others—part I, *Met. Finish.* 100 (2002) 9–19, [https://doi.org/10.1016/S0026-0576\(02\)80745-0](https://doi.org/10.1016/S0026-0576(02)80745-0).
- [30] S. Hörnström, E. Hedlund, H. Klang, J.O. Nilsson, M. Backlund, P.E. Tegehall, A surface study of the chemical pretreatment before coil coating of hot dip zinc-coated steel, *Surf. Interface Anal.* 19 (1992) 121–126, <https://doi.org/10.1002/sia.740190124>.
- [31] V. Saarimaa, C. Lange, T. Paunikallio, et al., Evaluation of surface activity of hot-dip galvanized steel after alkaline cleaning, *J. Coat. Technol. Res.* 17 (2020) 285–292, <https://doi.org/10.1007/s11998-019-00272-9>.
- [32] B.W. Çetinkaya, F. Junge, G. Müller, F. Haakmann, K. Schierbaum, M. Giza, Impact of alkaline and acid treatment on the surface chemistry of a hot-dip galvanized Zn–Al–Mg coating, *J. Mater. Res. Technol.* 9 (2020) 16445–16458, <https://doi.org/10.1016/j.jmrt.2020.11.070>.
- [33] Y.B. Makarychev, N.A. Gladkikh, G.V. Redkina, O.Y. Grafov, A.D. Aliev, Y. I. Kuznetsov, Formation of composite coatings on galvanized steel from organosilane solutions using electrophoresis and sol-gel technology, *Materials* 15 (2022) 2418.
- [34] P.R. Seré, W. Egli, A.R. Di Sarli, C. Deyá, Preparation and characterization of silanes films to protect electrogalvanized steel, *J. Mater. Eng. Perform.* 27 (2018) 1194–1202.
- [35] M. Fedel, M. Olivier, M. Poelman, F. Deflorian, S. Rossi, M.-E. Druart, Corrosion protection properties of silane pre-treated powder coated galvanized steel, *Prog. Org. Coat.* 66 (2009) 118–128, <https://doi.org/10.1016/j.porgcoat.2009.06.011>.
- [36] M. Yu, M. Liang, J. Liu, S. Li, B. Xue, H. Zhao, Effect of chelating agent acetylacetone on corrosion protection properties of silane-zirconium sol-gel coatings, *Appl. Surf. Sci.* 363 (2016) 229–239, <https://doi.org/10.1016/j.apsusc.2015.12.013>.
- [37] M. Taheri, R. Naderi, M. Mahdavian, Enhancement of corrosion resistance of mild steel in NaCl solution with an eco-friendly silane coating containing nanoclay and zinc acetylacetonate, *Pigment Resin Technol.* (2018), <https://doi.org/10.1108/PRT-12-2017-0108>.
- [38] R. Berger, U. Bexell, N. Stavlid, T.M. Grehk, The influence of alkali-degreasing on the chemical composition of hot-dip galvanized steel surfaces, *Surf. Interface Anal.* 38 (2006) 1130–1138, <https://doi.org/10.1002/sia.2364>.
- [39] B.A. Horri, M. Choolaei, A. Chaudhry, H. Qaali, A highly efficient hydrogen generation electrolysis system using alkaline zinc hydroxide solution, *Int. J. Hydrog. Energy* 44 (2019) 72–81, <https://doi.org/10.1016/j.ijhydene.2018.03.048>.
- [40] A. Salmasifar, M. Edraki, E. Alibakhshi, B. Ramezanzadeh, G. Bahlakeh, Theoretical design coupled with experimental study of the effectiveness of the inhibitive molecules based on Cynara scolymus L extract toward chloride-induced corrosion of steel, *J. Mol. Liq.* 332 (2021), 115742, <https://doi.org/10.1016/j.molliq.2021.115742>.
- [41] E. Alibakhshi, E. Ghasemi, M. Mahdavian, B. Ramezanzadeh, The effect of interlayer spacing on the inhibitor release capability of layered double hydroxide based nanocontainers, *J. Clean. Prod.* 251 (2020), 119676, <https://doi.org/10.1016/j.jclepro.2019.119676>.
- [42] E. Alibakhshi, E. Ghasemi, M. Mahdavian, B. Ramezanzadeh, A comparative study on corrosion inhibitive effect of nitrate and phosphate intercalated zn-Al-layered double hydroxides (LDHs) nanocontainers incorporated into a hybrid silane layer and their effect on cathodic delamination of epoxy topcoat, *Corros. Sci.* 115 (2017) 159–174, <https://doi.org/10.1016/j.corsci.2016.12.001>.
- [43] E. Callone, R. Ceccato, F. Deflorian, M. Fedel, S. Diré, Filler-matrix interaction in sodium montmorillonite-organosilica nanocomposite coatings for corrosion protection, *Appl. Clay Sci.* 150 (2017) 81–88.
- [44] R.C. Tan, J.Q. Vien, W. Wu, Hydrolysis of α -chloro-substituted 2-and 4-pyridones: rate enhancement by zwitterionic structure, *Bioorg. Med. Chem. Lett.* 22 (2012) 1224–1225.

- [45] M. Palimi, E. Alibakhshi, B. Ramezanzadeh, G. Bahlakeh, M. Mahdavian, Screening the anti-corrosion effect of a hybrid pigment based on zinc acetyl acetonate on the corrosion protection performance of an epoxy-ester polymeric coating, *J. Taiwan Inst. Chem. Eng.* 82 (2018) 261–272, <https://doi.org/10.1016/j.jtice.2017.10.014>.
- [46] M. Mahdavian, A.R. Tehrani-Bagha, E. Alibakhshi, et al., Corrosion of mild steel in hydrochloric acid solution in the presence of two cationic gemini surfactants with and without hydroxyl substituted spacers, *Corros. Sci.* 137 (2018) 62–75, <https://doi.org/10.1016/j.corsci.2018.03.034>.
- [47] S. Khamseh, E. Alibakhshi, B. Ramezanzadeh, et al., Tailoring hardness and electrochemical performance of TC4 coated Cu/aC thin coating with introducing second metal zr, *Corros. Sci.* 172 (2020), 108713, <https://doi.org/10.1016/j.corsci.2020.108713>.
- [48] M. Razizadeh, M. Mahdavian, B. Ramezanzadeh, E. Alibakhshi, S. Jamali, Synthesis of hybrid organic–inorganic inhibitive pigment based on basil extract and zinc cation for application in protective construction coatings, *Constr. Build. Mater.* 287 (2021), 123034, <https://doi.org/10.1016/j.conbuildmat.2021.123034>.
- [49] S. Khamseh, E. Alibakhshi, B. Ramezanzadeh, M.G. Sari, A tailored pulsed substrate bias voltage deposited (aC: Nb) thin-film coating on GTD-450 stainless steel: enhancing mechanical and corrosion protection characteristics, *Chem. Eng. J.* 404 (2021), 126490, <https://doi.org/10.1016/j.cej.2020.126490>.
- [50] S. Hiromoto, S. Itoh, K. Doi, H. Katayama, T. Akashi, Short-and long-term corrosion behavior of carbonate apatite-coated mg-4mass% Y-3mass% RE alloy in cell culture medium, *Corros. Sci.* 200 (2022), 110222.
- [51] R. Samiee, B. Ramezanzadeh, M. Mahdavian, E. Alibakhshi, G. Bahlakeh, Designing a non-hazardous nano-carrier based on graphene oxide@ polyaniline-praseodymium (III) for fabrication of the Active/Passive anti-corrosion coating, *J. Hazard. Mater.* 398 (2020), 123136, <https://doi.org/10.1016/j.jhazmat.2020.123136>.
- [52] R. Samiee, B. Ramezanzadeh, M. Mahdavian, E. Alibakhshi, G. Bahlakeh, Graphene oxide nano-sheets loading with praseodymium cations: adsorption-desorption study, quantum mechanics calculations and dual active-barrier effect for smart coatings fabrication, *J. Ind. Eng. Chem.* 78 (2019) 143–154, <https://doi.org/10.1016/j.jiec.2019.06.024>.
- [53] F. Marhamati, M. Mahdavian, S. Bazgir, Corrosion mitigation of mild steel in hydrochloric acid solution using grape seed extract, *Sci. Rep.* 11 (2021) 1–16, <https://doi.org/10.1038/s41598-021-97944-7>.
- [54] A. Khor, P. Leung, M. Mohamed, et al., Review of zinc-based hybrid flow batteries: from fundamentals to applications, *Mater. Today Energy.* 8 (2018) 80–108, <https://doi.org/10.1016/j.mtener.2017.12.012>.
- [55] J.-M.R. Génin, C. Ruby, A. Géhin, P. Refait, Synthesis of green rusts by oxidation of Fe (OH) 2, their products of oxidation and reduction of ferric oxyhydroxides; Eh–pH pourbaix diagrams, *Compt. Rendus Geosci.* 338 (2006) 433–446, <https://doi.org/10.1016/j.crte.2006.04.004>.
- [56] T. Moeller, *Chemistry: With Inorganic Qualitative Analysis*, Elsevier, 2012.
- [57] M.B. Smith, *Organic Synthesis*, 3rd ed, Elsevier, 2010.
- [58] M.E.H.N. Tehrani, M. Ramezanzadeh, B. Ramezanzadeh, A highly-effective/durable metal-organic anti-corrosion film deposition on mild steel utilizing Malva sylvestris (MS) phytoextract-divalent zinc cations, *J. Ind. Eng. Chem.* 95 (2021) 292–304, <https://doi.org/10.1016/j.jiec.2021.01.002>.
- [59] M. Keramatinia, M. Ramezanzadeh, G. Bahlakeh, B. Ramezanzadeh, Synthesis of a multi-functional zinc-centered nitrogen-rich graphene-like thin film from natural sources on the steel surface for achieving superior anti-corrosion properties, *Corros. Sci.* 178 (2021), 109077, <https://doi.org/10.1016/j.corsci.2020.109077>.
- [60] H. Ferkous, B. Talhi, M. Barj, R. Boukherroub, S. Szunerits, Investigation of the ability of the corrosion protection of zn-mg coatings, *Open Corros. J.* 2 (2009), <https://doi.org/10.2174/1876503300902010026>.
- [61] P.C. Banerjee, R.S. Raman, Electrochemical impedance spectroscopic investigation of the role of alkaline pre-treatment in corrosion resistance of a silane coating on magnesium alloy, ZE41, *Electrochim. Acta* 56 (2011) 3790–3798, <https://doi.org/10.1016/j.electacta.2011.02.050>.
- [62] L. Palomino, I. Aquino, I. Aoki, H.De Melo, *EIS Investigation of the Behaviour in 0.1 M Sodium Chloride Solution of a Double Layer Cerium–Silane Pre-treatment on Al 2024-T3*, Woodhead Publishing, 2007.
- [63] Q. Zhao, W. Guo, Q. Zhong, J. Zhang, J. Sun, H. Li, The electrochemical behavior of doped silane pre-treatments on galvanized steel substrates, *Surf. Rev. Lett.* 24 (2017) 1750015, <https://doi.org/10.1142/S0218625X17500159>.